Quantum particle in a split box: Excitations to the ground state

Vegard B. Sørdal and Joakim Bergli
Department of Physics, University of Oslo, 0316 Oslo, Norway

(Received 11 December 2018; published 20 February 2019)

We discuss two different approaches for splitting the wave function of a single-particle box (SPB) into two equal parts. Adiabatic insertion of a barrier in the center of a SPB in order to make two compartments which each have probability $1/2$ of finding the particle in it is one of the key steps for a Szilard engine. However, any asymmetry between the volume of the compartments due to an off-center insertion of the barrier results in a particle that is fully localized in the larger compartment, in the adiabatic limit. We show that rather than exactly splitting the eigenfunctions in half by a symmetric barrier, one can use a nonadiabatic insertion of an asymmetric barrier to induce excitations to only the first excited state of the full box. As the barrier strength goes to infinity the excited state of the full box becomes the ground state of one of the new boxes. Thus, we can achieve close to exact splitting of the probability between the two compartments using the more realistic nonadiabatic, not perfectly centered barrier, rather than the idealized adiabatic and central barrier normally assumed.

DOI: 10.1103/PhysRevA.99.022121

I. INTRODUCTION

The Szilard engine is a simple conceptual model of an information processing system [1]. The classical model is a single particle in a box, coupled to a thermal bath. By inserting a movable barrier in the center of the box, the probability of finding the particle in either compartment becomes $1/2$. If we now perform a measurement to find out which compartment the particle is in, we generate one bit of Shannon information which is stored in some memory. Since the box is coupled to a thermal bath, we can extract work by allowing the compartment in which we find the particle to expand and fill the whole box. The maximum work extracted in this way is $k_BT \ln 2$, and this is achieved by isothermal expansion. To complete the cycle the memory is deleted, which has a minimum energy cost of $k_BT \ln 2$, according to Landauer's principle [2]. Therefore, if we perform reversible operations, the full cycle of measurement, work extraction, and information deletion generates no entropy. The quantum mechanical version of the Szilard engine is similar, only now we are splitting the wave function of the particle. The quantum measurement and, assuming the memory is classical, deletion is similar to the classical case, but there are subtle differences when it comes to the insertion, expansion, and removal of the barrier [3].

The adiabatic theorem in quantum mechanics tells us that a system remains in its instantaneous eigenstate as long as it has a gapped energy spectrum and the perturbation acting on it is slow enough to prevent transition between the eigenstates. Based on this, it has been remarked in [4] that if the particle is in the ground state and the barrier is inserted off-center, such that one compartment is larger than the other, the particle will always be localized in the larger compartment. This is because the energy spectrum is proportional to L^{-2}, where L is the length of the compartment. The result is independent of how small the asymmetry between the compartments is; any finite difference between the compartment sizes will give the same result.

With modern technology we can now experimentally realize what was before only a thought experiment. In the last decade, the creation of Szilard engines has been reported in a range of physical systems: atoms [5–7], colloidal particles [8,9], molecules [10], electrons [11–13], and photons [14]. In experiments the barrier is not inserted adiabatically nor exactly in the center, and one can ask the question of how the result of the previous paragraph changes when the barrier is inserted at a finite rate.

Although a finite rate of insertion can make the probability of finding the particle in the smaller compartment nonzero, the downside is that a fast rate results in excitations to higher energy levels. The Szilard engine measurement procedure traditionally only determines which side of the box the particle is found, not its exact eigenstate. Therefore excitation of high energy states introduces additional entropy that is not accounted for in the which-side measurement. Information is therefore lost when performing the measurement, leading to decreased efficiency of the Szilard engine.

Previous work [15] has studied the asymmetric insertion of a δ potential barrier at high rates of insertion. In contrast to their work, we expand the full wave function in its instantaneous energy eigenstates and point out the fact that it is possible to asymmetrically insert a barrier with a finite rate and obtain very close to an equal probability distribution, with negligible excitations to higher states than to the first excited state. Therefore, the asymmetric Szilard engine with finite rate of insertion of the barrier can have the same efficiency as the symmetric Szilard engine with adiabatic insertion.

There are two fundamentally different ways to get an equal probability of occupying the left and right box of a Szilard engine. One way is to follow the usual protocol of splitting a symmetric wave function into two exactly equal parts, i.e., inserting a barrier in the center of a box with a particle in the ground state. Figure 1 shows the time evolution of the eigenstates and eigenenergies when inserting a barrier with time-dependent strength $\alpha(t)$ (dashed vertical line), in the

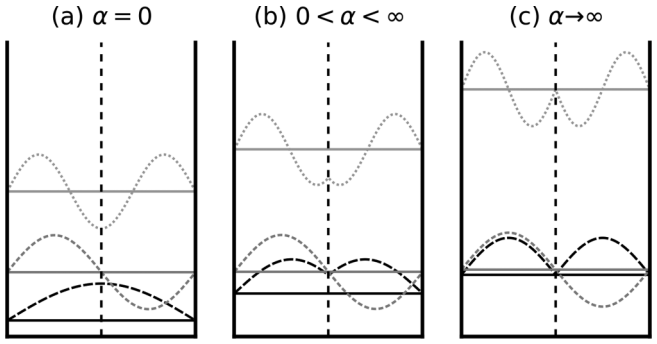

FIG. 1. Schematic of the three first eigenfunction and energies for a symmetric box for three different values of the barrier strength $\alpha(t)$. (a) Initial state of the system, before the barrier is inserted. (b) At an intermediate time before $\alpha(t) \to \infty$. We see that when the barrier is inserted at the center of the box it hits the nodes of the antisymmetric eigenfunctions, and therefore there are no excitations to this state [see Eq. (6)]. (c) The limit when $\alpha(t) \to \infty$. The total wave function is symmetric about the barrier, and the probability of finding the particle in either compartment is $1/2$.

center of the box. Figure 1(a) is the initial state of the system, before the barrier has begun to be inserted. Figure 1(b) is an intermediate step with $0 < \alpha < \infty$ before the two compartments have been completely isolated from each other in Fig. 1(c) as $\alpha \to \infty$. The eigenstates in Fig. 1(c) are split exactly in half, with a probability of $1/2$ on either side.

The second way is to insert the barrier asymmetrically and nonadiabatically, in such a way that only the first excited state is excited; the eigenfunction of the ground state will be large in the larger compartment and small in the smaller compartment, and vice versa for the first excited state. This method is illustrated in Fig 2. The initial state in Fig. 2(a), before the barrier is inserted, is identical to that in Fig. 1(a). However, as the barrier is increased via 2(b) through 2(c) the symmetric eigenfunction becomes zero in the smaller compartment, while the antisymmetric becomes zero in the larger compartment. Of course it has to be this way, since when

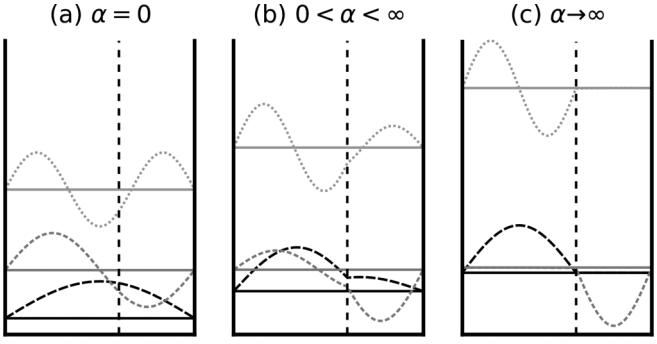

FIG. 2. Same as Fig. 1(a), but for an asymmetric box. (a) The initial state of the system, identical to Fig. 1(a). Only now the eigenfunction of the first excited state is nonzero at the point we insert the barrier, allowing excitations from the ground state. From the intermediate time step in (b) to the final state in (c) the eigenfunction of the ground and first excited states evolves such that it is approximately zero in the smaller and larger compartments, respectively.

$\alpha \to \infty$ what we have is essentially two rescaled copies of the initial state. The third energy level in Fig. 2(a) becomes the new first excited state of the larger compartment in Fig. 2(c), while the first exited state in Fig. 2(a) becomes the new ground state of the smaller compartment in Fig. 2(c). Only exciting the first excited state of the original box still results in no excitations after the measurement, since it becomes the new ground state of the compartment.

A good thought experiment is never set in some complicated system with many degrees of freedom. Rather, it is a surprising result or counterintuitive implication obtained from the study of a simplified model of reality. One might ask why further study of a thought experiment that has already been experimentally realized is necessary. In our opinion there are two main reasons: The first reason is that studying all the aspects of this conceptual model helps us to understand the key physical effects that gave rise to the thought experiment in the first place, and guides us in how to think about their order of importance. The second reason is that even though thought experiments can guide our understanding regardless of whether it is possible to experimentally perform them, it is also important to investigate whether they present practical possibilities. They can act as benchmarks for testing how well one can control the heat and entropy flow in experiments, with the goal being to minimize heat waste in electronics. The Szilard engine, with its measurement and memory scheme, is ideal in this sense.

In the rest of this article we address the two following questions related to how we can limit excitations to the first excited level only, using a simple protocol for the barrier insertion: How sensitive is the nonadiabatic splitting of the wave function to asymmetry in barrier insertion, and what is the probability of exciting states higher than the lowest two when we insert the barrier with a finite rate.

II. ANALYSIS

The box is shown in Fig. 2 and is defined by the potential $V(x) = 0$ for $x \in [-a, b]$ and $V(x) = \infty$ elsewhere. The barrier is a δ function with time-dependent strength $\alpha(t)$ inserted at $x = 0$. We choose the barrier to be a δ function since it allows presenting the eigenstates in analytical form. A barrier with finite width was used in [4], while in [15] they used a δ function barrier and obtained similar results. The width of the barrier would only affect the tunneling rate between the compartments, but the qualitative results would remain unchanged. The insertion of the barrier is described by a time-dependent Hamiltonian given by

$$\hat{H}(t) = -\frac{\hbar^2}{2m}\frac{\partial^2}{\partial x^2} + \alpha(t)\delta(x), \tag{1}$$

where m is the mass of the particle. The instantaneous eigenfunctions $|\psi_n(t)\rangle$ that evolve are found as the solution to the time-independent Schrödinger equation

$$\hat{H}(t)\,|\psi_n(t)\rangle = E(t)\,|\psi_n(t)\rangle\,. \tag{2}$$

At any given time the instantaneous eigenfunctions is an orthonormal set $\langle\psi_n|\psi_m\rangle = \delta_{n,m}$. Therefore the total wave function $|\Psi(t)\rangle$, which is the solution of the time-dependent

Schrödinger equation

$$i\hbar\,\partial_t\,|\Psi(t)\rangle = \hat{H}\,|\Psi(t)\rangle\,, \tag{3}$$

can be expressed as a linear combination of them

$$|\Psi(t)\rangle = \sum_n c_n(t)\,|\psi_n(t)\rangle\,e^{i\theta_n(t)}, \quad \theta_n = -\frac{1}{\hbar}\int_0^t E_n(t')dt'. \tag{4}$$

Here $c_n(t)$ is a set of complex constants satisfying $\sum_n^\infty |c_n(t)|^2 = 1$. As shown in Appendix A, the system of coupled differential equations giving the time evolution of the coefficients $\{c_n\}$ is

$$\dot{c}_n(t) = -\sum_{m\neq n} c_m(t)\frac{\langle\psi_n(t)|\partial_t\hat{H}|\psi_m(t)\rangle}{E_m - E_n}e^{i(\theta_m-\theta_n)}. \tag{5}$$

We first need to find the instantaneous solutions $|\psi_n(t)\rangle$ for the asymmetric barrier problem, and the details of these calculations are given in Appendix B. After finding the instantaneous solutions we numerically solve Eq. (5) to find the time evolution of $|\Psi(t)\rangle$.

III. RESULTS

Let us now see to what extent it is possible to make the probability of finding the particle in either compartment equal (or as close to equal as possible), while limiting excitations to higher energy states.

We set the total length of the box equal to $L = a + b = 1$, and define $a = 1/2 + \epsilon$, where ϵ is the asymmetry parameter that determines how much larger the compartment on the left side of the barrier is than the one on the right side. We also set $\hbar = m = 1$. The initial state is chosen to be the ground state, which is $c_1(0) = 1$ and $c_n(0) = 0$ for $n > 1$. We found that including the six first eigenstates was sufficient to capture all the excitations for the insertion rates we explored. We set the maximum strength of the barrier at the end of the protocol ($t = \tau$) to $\alpha(\tau) = 400\,E_0$, where E_0 is the ground state of the box of $L = 1$ without a barrier. This value was chosen to make sure that the coefficients $\{c_n(\tau)\}$ converged to constant values.

For the protocol we chose $\alpha(t) = At^2$, where A is some constant that determines the rate of insertion. We also tried a linear protocol, but found that in order to limit higher-order excitation the rate of insertion had to start small and steadily increase as a function of time. The reason for this can be understood by studying the coupling between the $\{c_n(t)\}$ in Eq. (5) at a given time t

$$\frac{\langle\psi_n(t)|\partial_t\hat{H}|\psi_m(t)\rangle}{E_m - E_n} = \dot{\alpha}(t)\frac{\langle\psi_n(t)|\hat{\delta}(x)|\psi_m(t)\rangle}{E_m - E_n}. \tag{6}$$

When we insert the barrier, the probability of finding the particle at the insertion point decreases in proportion to the strength of the barrier. Therefore the numerator, $\langle\psi_n(t)|\hat{\delta}(x)|\psi_m(t)\rangle$, which measures overlap between the eigenstates at the insertion point, will be largest in the beginning and decrease toward zero as the barrier strength is increased. This prevents transitions for high barriers. The denominator is the energy difference between the eigenstates, $E_m - E_n$, and its dependence on the barrier strength is shown in Fig. 3. The energy difference between the ground state and the first exited state is largest in the beginning and asymptotically approaches a final small value that increases with the asymmetry between the compartments. This makes transition between these more likely as the barrier strength increases.

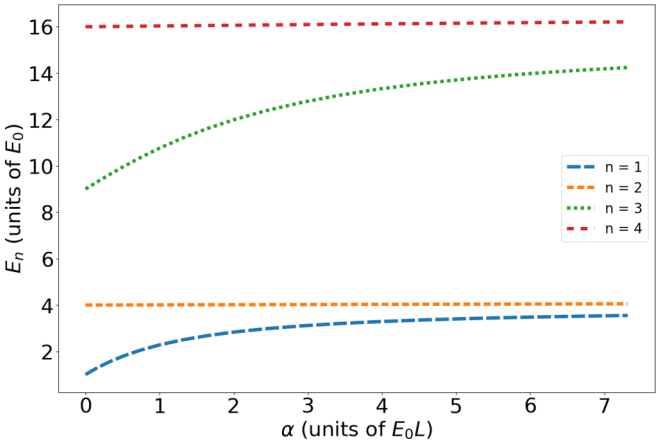

FIG. 3. Energy levels as a function of time. We see that the odd energy levels approach the evens as the strength of the barrier increases, and the final spacing between them decreases with the magnitude of the asymmetry.

In Fig. 4 we plot the ratio $\langle\psi_1(t)|\hat{\delta}(x)|\psi_m(t)\rangle\,/(E_m - E_1)$ and interpret its magnitude as an indication of the coupling strength between the ground state and the mth eigenstate. As argued in the previous paragraph we see that indeed the ground state's coupling to the first excited state dominates over its coupling to other eigenstates once the barrier has reached a certain strength ($\simeq 4\,E_0$ in this example, where $\epsilon = 0.1$). As seen in Eq. (6), we can control the coupling strength via $\dot{\alpha}(t)$. By choosing a $\dot{\alpha}(t)$ that is small in the beginning and large toward the end of the protocol, we suppress early

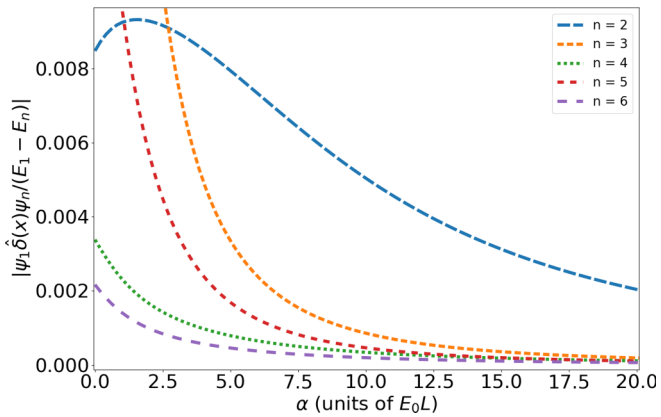

FIG. 4. Dependence of the ratio $\frac{\langle\psi_1(t)|\hat{\delta}(x)|\psi_m(t)\rangle}{E_m - E_1}$ on the strength of the barrier α. Its magnitude gives us an indication of the coupling between the ground state and the higher excited states. We see that the coupling between the ground state and the first excited state remains substantial for high values of α, while all the others decay quickly. This indicates that we can induce transitions between those two levels without exciting higher states when α is large. This plot was obtained with $\epsilon = 0.1$.

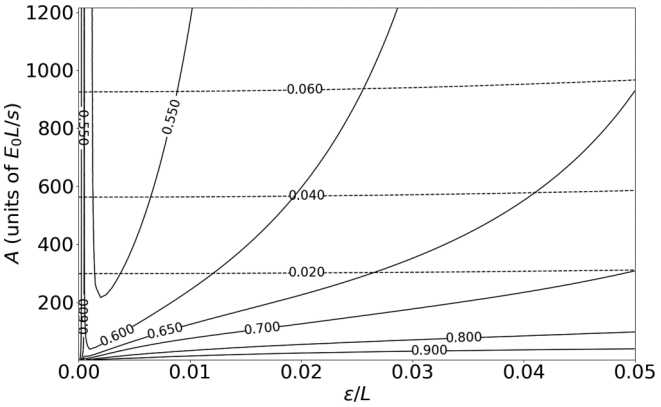

FIG. 5. Probability of finding the particle in the largest compartment (solid lines), as a function of the barrier insertion rate constant A and the asymmetry parameter ϵ. The probability to excite levels higher than the first excited state is shown in the dashed lines.

transitions between the levels when $\langle\psi_n(t)|\hat{\delta}(x)|\psi_m(t)\rangle/(E_m - E_n)$ is large. Since the energy difference between the ground state and the first excited state becomes much smaller than the difference between the ground state and any of the higher states, we can induce transitions between them, even when the wave function overlap is very small, if we choose a $\dot{\alpha}(t)$ that is suitably large.

In Fig. 5 we show a contour plot of the probability of finding the particle in the bigger compartment (solid lines) at the end of the protocol as a function of the asymmetry parameter ϵ/L and the insertion rate parameter A. We see that even for asymmetries of the order of $\epsilon \sim 0.01$ the probability of finding the particle in the bigger compartment is quite large. Although increasing the barrier faster makes the probabilities of finding the particle in either side more equal it also incurs a penalty; the faster you increase the barrier the more likely it is that you excite higher-order states in the energy spectrum. Higher-order excitations increases the entropy of the system, since the internal states of the Szilard engine are assumed to be either the ground state (bigger compartment) or the first excited state (smaller compartment).

IV. SUMMARY AND DISCUSSION

When designing a Szilard engine one wants the probabilities of finding the particle in either compartment after barrier insertion to be equal. Experimentally it might be difficult to design a perfectly symmetric double-well potential. We point out the fact that excitations to the first excited state are special in the sense that after the barrier strength becomes high enough to stop tunneling between the two compartments, and a measurement to determine which compartment the particle is found is performed, the system is still in the ground state for the relevant compartment. This is a generic result, but exactly how to limit the excitations to only the first excited state depends on the specific protocol $\alpha(t)$. We have used a simple protocol that is quadratic in time as an example, and investigated how sensitive the probability distribution of the divided single-particle box is to asymmetry between the compartment size. We find that for this protocol even small differences between the width of the compartments, results in a probability distribution that is skewed toward the larger compartment. The faster one increases the barrier strength, the more even the final distribution becomes. However, this rapid increase also leads to higher-order excitations in the box, which results in unwanted entropy production. The question remains whether a protocol can be constructed such that it gives an equal final distribution between the left and right side, and how sensitive it is to variations in the asymmetry.

ACKNOWLEDGMENT

We thank Y. M. Galperin for valuable discussions and comments on the manuscript.

APPENDIX A: WAVE FUNCTION FOR TIME-DEPENDENT HAMILTONIAN

In this section we follow [16] (Sec. 10.1.2) and write the total wave function $|\Psi(t)\rangle$ as a linear combination of the instantaneous eigenstates $|\psi(t)_n\rangle$ and derive the coupled differential equation for the coefficients. When the Hamiltonian changes with time, the eigenfunctions and eigenvalues are also time dependent,

$$\hat{H}(t)\,|\psi_n(t)\rangle = E_n(t)\,|\psi_n(t)\rangle\,. \tag{A1}$$

The eigenfunctions at any given time is an orthonormal set, $\langle\psi_n(t)|\psi_m(t)\rangle = \delta_{n,m}$, and the total wave function which can be found as the solution of the time-dependent Schrödinger equation

$$i\hbar\,\partial_t\,|\Psi(t)\rangle = \hat{H}\,|\Psi(t)\rangle \tag{A2}$$

can be expressed as a linear combination of them:

$$|\Psi(t)\rangle = \sum_n c_n(t)\,|\psi_n(t)\rangle\,e^{i\theta_n(t)}, \tag{A3}$$

where

$$\theta_n = -\frac{1}{\hbar}\int_0^t E_n(t')dt'. \tag{A4}$$

Inserting this linear combination into the time-dependent Schrödinger equation gives us

$$i\hbar\textstyle\sum_n[\dot{c}_n\,|\psi_n\rangle + c_n\,|\dot{\psi}_n\rangle + ic_n\,|\psi_n\rangle\,\dot{\theta}_n]e^{i\theta_n} \tag{A5}$$

$$= \textstyle\sum_n c_n\hat{H}\,|\psi_n\rangle\,e^{i\theta_n}. \tag{A6}$$

Now since $\dot{\theta}_n = -E_n/\hbar$ and $\hat{H}\,|\psi_n\rangle = E_n\,|\psi_n\rangle$, the right-hand side exactly cancels the last term on the left-hand side and we are left with

$$\sum_n[\dot{c}_n\,|\psi_n\rangle + c_n\,|\dot{\psi}_n\rangle]e^{i\theta_n} = 0. \tag{A7}$$

We now take the inner product with the eigenfunction ψ_m, and since the eigenfunctions constitute an orthonormal set at any given time t, we obtain a set of N coupled differential equations for the N coefficients c_n, $n \in [1, N]$.

$$\sum_n[\dot{c}_n\delta_{m,n} + c_n\,\langle\psi_m|\dot{\psi}_n\rangle]e^{i\theta} = 0, \tag{A8}$$

$$\dot{c}_m(t) = -\sum_n c_n\,\langle\psi_m|\dot{\psi}_n\rangle\,e^{i(\theta_n-\theta_m)}. \tag{A9}$$

We can rewrite this equation by taking the time derivative of Eq. (A1) and then the inner product with ψ_m to obtain

$$\langle\psi_m|\dot{\hat{H}}|\psi_n\rangle + E_m\langle\psi_m|\dot{\psi}_n\rangle = \dot{E}\delta_{m,n} + E_n\langle\psi_m|\dot{\psi}_n\rangle, \quad \text{(A10)}$$

which shows us that the inner product $\langle\psi_m|\dot{\psi}_n\rangle$ can be written as

$$\langle\psi_m|\dot{\psi}_n\rangle = \frac{\langle\psi_m|\dot{\hat{H}}|\psi_n\rangle}{E_n - E_m}, \quad \text{(A11)}$$

as long as the system is nondegenerate and $n \neq m$. Putting this result into Eq. (A9) we get

$$\dot{c}_m = -c_m\langle\psi_m|\dot{\psi}_m\rangle - \sum_{n\neq m} c_n \frac{\langle\psi_m|\dot{\hat{H}}|\psi_n\rangle}{E_n - E_m} e^{i(\theta_n-\theta_m)}. \quad \text{(A12)}$$

This form of the differential equation is particularly well suited to our problem. First, the Hamiltonian contains a δ function at $x = 0$, so the integral $\langle\psi_m|\dot{\hat{H}}|\psi_n\rangle$ is simply given by (using the eigenfunctions from Appendix B)

$$\langle\psi_m|\dot{\hat{H}}|\psi_n\rangle = \dot{\alpha}A_nA_m\sin(k_na)\sin(k_ma). \quad \text{(A13)}$$

In addition, the term $\langle\psi_m|\dot{\psi}_m\rangle$ is always zero. This is because the instantaneous eigenfunctions $|\psi_m\rangle$ are orthonormal ($\langle\psi_m|\psi_m\rangle = 1$) and real:

$$\frac{\partial}{\partial t}\langle\psi_m|\psi_m\rangle = \langle\dot{\psi}_m|\psi_m\rangle + \langle\psi_m|\dot{\psi}_m\rangle = 0. \quad \text{(A14)}$$

Since $\langle\psi_m|\dot{\psi}_m\rangle = \langle\dot{\psi}_m|\psi_m\rangle^*$ we get

$$\langle\psi_m|\dot{\psi}_m\rangle = -\langle\psi_m|\dot{\psi}_m\rangle^* \rightarrow \mathrm{Re}[\langle\psi_m|\dot{\psi}_m\rangle] = 0. \quad \text{(A15)}$$

Therefore the coupled differential equations we need to solve become

$$\dot{c}_m = -\sum_{n\neq m} c_n \frac{\langle\psi_m|\dot{\hat{H}}|\psi_n\rangle}{E_n - E_m} e^{i(\theta_n-\theta_m)}. \quad \text{(A16)}$$

APPENDIX B: ASYMMETRIC BARRIER

We can find the stationary states from the time-independent Schrödinger equation and they have the form

$$\psi(x) = \begin{cases} A\sin[k(x+a)], & x \in [-a, 0], \\ B\sin[k(x-b)], & x \in [0, b], \end{cases} \quad \text{(B1)}$$

where $k = \sqrt{2mE}/\hbar$. At $x = 0$ the wave function is continuous while its derivative has a discontinuity. These two conditions are

$$\lim_{\epsilon\to 0}[\psi(0-\epsilon) - \psi(0+\epsilon)] = 0, \quad \text{(B2)}$$

$$\lim_{\epsilon\to 0}[\dot{\psi}(0+\epsilon) - \dot{\psi}(0-\epsilon)] = \frac{2m\alpha}{\hbar^2}\psi(0), \quad \text{(B3)}$$

and for our system they result in

$$A\sin(ka) = -B\sin(kb), \quad \text{(B4)}$$

$$B\cos(kb) - A\cos(ka) = \frac{2m\alpha}{k\hbar^2}A\sin(ka). \quad \text{(B5)}$$

Combining these equations gives us another one, which we can solve numerically to find the wave vectors k for a given a, b, and α.

$$\sin[k(a+b)] = -\frac{2m\alpha}{k\hbar^2}\sin(ka)\sin(kb). \quad \text{(B6)}$$

The solutions to this equation defines a discrete set of allowed values for the wave vector $k \rightarrow k_n$, $n = 1, 2, \ldots$, which determines the energy spectrum of the system via

$$E_n = \frac{\hbar}{2m}k_n^2. \quad \text{(B7)}$$

The wave function has to be normalized on the domain of x,

$$\int_{-a}^{0} A_n^2\sin^2[k_n(x+a)] + \int_0^b B_n^2\sin^2[k_n(x-b)] = 1, \quad \text{(B8)}$$

which combined with Eq. (B4) gives us the normalization constants A_n

$$A_n^2 = \left[\frac{a}{2} - \frac{\sin(2k_na)}{4k_n} + \frac{\sin^2(k_na)}{\sin^2(k_nb)}\left(\frac{b}{2} - \frac{\sin(2k_nb)}{4k_n}\right)\right]^{-1}. \quad \text{(B9)}$$

B_n can be found via Eq. (B4).

[1] L. Szilard, Über die entropieverminderung in einem thermodynamischen system bei eingriffen intelligenter wesen, Z. Phys. **53**, 840 (1929).

[2] R. Landauer, Irreversibility and heat generation in the computing process, IBM J. Res. Dev. **5**, 183 (1961).

[3] S. W. Kim, T. Sagawa, S. De Liberato, and M. Ueda, Quantum Szilard Engine, Phys. Rev. Lett. **106**, 070401 (2011).

[4] J. Gea-Banacloche, Splitting the wave function of a particle in a box, Am J. Phys. **70.3**, 307 (2002).

[5] G. N. Price, S. T. Bannerman, K. Viering, E. Narevicius, and M. G. Raizen, Single-Photon Atomic Cooling, Phys. Rev. Lett. **100**, 093004 (2008).

[6] J. J. Thorn, E. A. Schoene, T. Li, and D. A. Steck, Experimental Realization of an Optical One-Way Barrier for Neutral Atoms, Phys. Rev. Lett. **100**, 240407 (2008).

[7] M. G. Raizen, Comprehensive control of atomic motion, Science **324**, 1403 (2009).

[8] S. Toyabe, T. Sagawa, M. Ueda, E. Muneyuki, and M. Sano, Experimental demonstration of information-to-energy conversion and validation of the generalized Jarzynski equality, Nat. Phys. **6**, 988 (2010).

[9] A. Berut, A. Arakelyan, A. Petrosyan, S. Ciliberto, R. Dillenschneider, and E. Lutz, Experimental verification of Landauer's principle linking information and thermodynamics, Nature **483**, 187 (2012).

[10] V. Serreli, C.-F. Lee, E. R. Kay, and D. A Leigh, A molecular information ratchet, Nature **445**, 523 (2007).

[11] J. V. Koski, V. F. Maisi, J. P. Pekola, and D. V. Averin, Experimental realization of a Szilard engine with a single electron, PNAS **111**, 13786 (2014).

[12] J. V. Koski, A. Kutvonen, I. M. Khaymovich, T. Ala-Nissila, and J. P. Pekola, On-Chip Maxwell's Demon as an Information-Powered Refrigerator, Phys. Rev. Lett. **115**, 260602 (2015).

[13] K. Chida, K. Nishiguchi, G. Yamahata, H. Tanaka, and A. Fujiwara, Thermal-noise suppression in nano-scale Si field-effect transistors by feedback control based on single-electron detection, Appl. Phys. Lett. **107**, 073110 (2015).

[14] M. D. Vidrighin, O. Dahlsten, M. Barbieri, M. S. Kim, V. Vedral, and I. A. Walmsley, Photonic Maxwell's Demon, Phys. Rev. Lett. **116**, 050401 (2016).

[15] S. K. Baek, S. D. Yi, and M. Kim, Particle in a box with a time-dependent δ-function potential, Phys. Rev. A **94**, 052124 (2016).

[16] D. J. Griffiths and D. F. Schroeter, *Introduction to Quantum Mechanics*, 3rd ed. (Cambridge University, New York, 2018).